AJNR

Magnetic Resonance Imaging of the Cervical Spine: Technical and Clinical Observations

Michael T. Modic, Meredith A. Weinstein, William Pavlicek, Francis Boumphrey, Daniel Starnes and Paul M. Duchesneau

AJNR Am J Neuroradiol 1984, 5 (1) 15-22
http://www.ajnr.org/content/5/1/15

Magnetic Resonance Imaging of the Cervical Spine: Technical and Clinical Observations

Michael T. Modic[1]
Meredith A. Weinstein[1]
William Pavlicek[1]
Francis Boumphrey[2]
Daniel Starnes[1]
Paul M. Duchesneau[1]

Seventy-two patients were examined to determine the clinical potential for magnetic resonance imaging (MRI) of the spine. MRI using different pulse sequences was compared with plain radiography, high-resolution computed tomography, and myelography. There were 35 normal patients; pathologic conditions studied included canal stenosis, herniated disk, metastatic tumor, neurofibroma, trauma, Chiari malformation, syringomyelia, arteriovenous malformation, and rheumatoid arthritis. MRI provided sharply defined anatomic delineation and tissue characterization. It was diagnostic in syringomyelia and Chiari malformation and was useful in the evaluation of trauma and spinal canal block from any cause. MRI was sensitive to degenerative disk disease and infection. The spin-echo technique, with three pulse sequence variations, seems very promising. A short echo time (TE) produces the best signal-to-noise ratio and spatial resolution. Lengthening the TE enhances differentiation of various tissues by their signal intensity, while the combined increase of TE and recovery time (TR) produces selective enhancement of the cerebrospinal fluid signal intensity.

Early clinical experience with magnetic resonance imaging (MRI) has demonstrated its potential in the evaluation of the spine and foramen magnum [1–5]. With appropriate pulse-sequence technique, the spinal cord, brainstem, cerebrospinal fluid (CSF), and extradural structures such as the intervertebral disk have been depicted without the use of intrathecal contrast or ionizing radiation. We evaluated different magnetic resonance pulse sequences and compared the images with myelograms, CT scans, and plain radiographs of the cervical spine.

Subjects and Methods

Seventy-two patients formed the subject group for this study. Thirty-seven patients were studied for known or suspected disease of the cervical spine and foramen magnum. Thirty-five patients were studied as normal controls.

The basic method was a spin-echo technique using an echo time (TE) of 30 msec and a recovery time (TR) of 0.5 sec (formerly called saturation recovery). All patients were examined with this technique. Spin-echo images having a TE of 60 msec and a TR of 1 sec also were obtained in 14 cases. In five patients, spin-echo images with variations of TE (30, 60, 120 msec) and TR (0.5, 1, 2 sec) were obtained. Inversion-recovery images having an inversion pulse time (TI) of 450 msec between the 180° and 90° pulses and 1.5 sec TR were obtained in five cases.

Forty patients were studied with a 0.15 T resistive unit (Teslacon, Technicare). The total scan time for the spin-echo technique was related to the TR. With 0.5 sec TR, it was 4.5 min; with 1 sec TR, it was 8 min. For the inversion-recovery images with 1.5 sec TR, the scan time was 8 min. Twenty-eight patients were studied with a 0.3 T superconductive unit (Teslacon), and total scan times for the spin-echo images were 2.6 min for 0.5 sec TR and 4 min for 1 sec TR. Inversion-recovery images with 1.5 sec TR took 4.5 min. Four patients were studied with a 0.5 T superconductive unit (Teslacon). All three units are whole-body imaging systems (100-cm bore) that provide a nominal 1.5-cm slice thickness with all pulse techniques.

This article appears in the December 1983 issue of *AJR* and the January/February 1984 issue of *AJNR*.

Received July 19, 1983; accepted August 1, 1983.

Presented in part at the annual meeting of the American Roentgen Ray Society, Atlanta, April 1983.

[1] Department of Radiology, Cleveland Clinic Foundation, 9500 Euclid Ave., Cleveland, OH 44106. Address reprint requests to M. T. Modic.

[2] Department of Orthopedic Surgery, Cleveland Clinic Foundation, Cleveland, OH 44106.

***AJNR* 5:15–22, January/February 1984**
0195–6108/84/0501–0015 $00.00

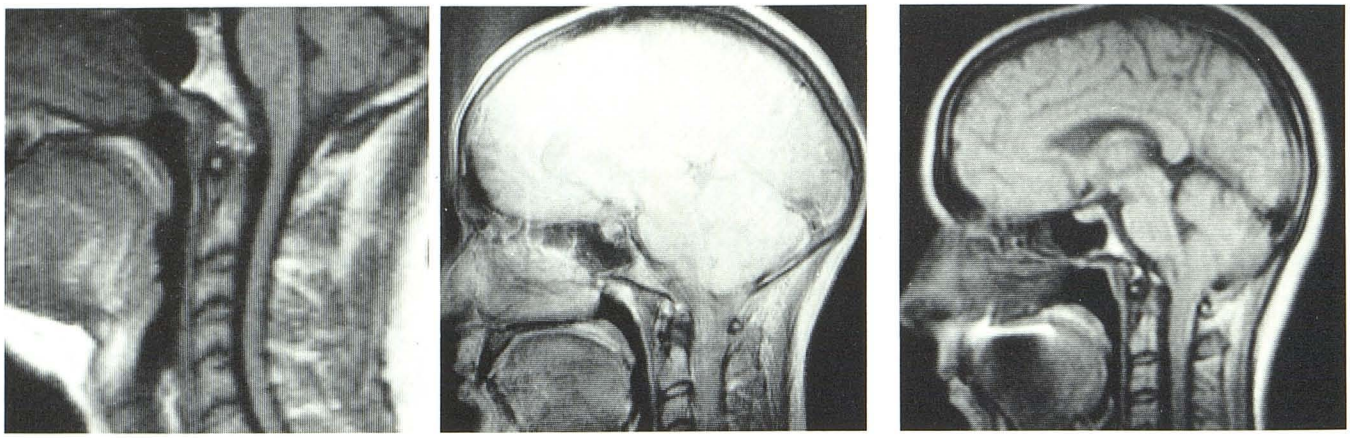

A B

Fig. 1.—Normal subjects. **A**, Spin-echo image (30 msec TE, 0.5 sec TR, 0.5 T superconductive unit) in sagittal plane of cervical spine and skull base. **B**, Spin-echo image (30 msec TE, 2.5 sec TR, 0.5 T superconductive unit) through head and upper cervical spine. Increased intensity of CSF space sharply delineating its outline but obscuring spinal cord. Low-intensity lesion incidentally noted in pituitary gland thought to represent adenoma.

Fig. 2.—Chiari I malformation. Spin-echo image (30 msec TE, 0.5 sec TR, 0.5 T superconductive unit). Herniation of cerebellar tonsils.

All images were reconstructed via two-dimensional Fourier methods to retrieve the phase-encoded positional information. Head and whole-body nuclear magnetic resonance coils were available for the units. The head coil was used for the foramen magnum and as much of the cervical spine as possible. The body coil was used for the lower cervical spine.

Observations

Normal

Thirty-five patients were studied as normal controls. Ten patients had correlative CT scans and/or myelograms that were normal. The fourth ventricle, cervical medullary junction, and cerebellar tonsils, and their relation to the foramen magnum, were delineated clearly in all cases. The level of the foramen magnum anteriorly was demarcated by a high spinal intensity representing fat just superior to the dens. Various high signal intensities from the lipid content within the marrow were seen in the clivus and occipital bone. The posterior rim of the foramen magnum was not as consistently localized because the lip of occipital cortical bone, which does not produce a magnetic resonance signal, was more variable in size posteriorly. Minimal soft-tissue thickening was identified posterior to the dens on the sagittal images, representing a combination of the synovial joint and the transverse ligament. The dens of C2 had a decreased signal compared with the adjacent vertebral body. A high-intensity signal from the marrow within the anterior arch of C1 was demarcated anterior to the dens. This is surrounded by cortical bone from which no signal is emitted (fig. 1A).

Spin-echo images (30 msec TE, 0.5 sec TR) in the head coil provided the best signal-to-noise ratio for the same scan time and the best contrast differentiation between the CSF and soft-tissue structures, such as the spinal cord. The intensity of the normal cervical disk is homogeneous with this technique. The central part of the cervical disk, in comparison with the periphery, shows a subtle increased signal intensity when the TE is increased to 60 or 120 msec. Increases in TR or TE result in a relative increase in the signal intensity of the CSF in relation to the cord and extradural structures. While this could prevent differentiation of the cord from CSF, it clearly delineates the subarachnoid space in relation to the extradural structures (fig. 1B).

Inversion-recovery images obtained in the same total scan time produced images of overall decreased signal intensity of the cord and disk tissue, and differentiation from the CSF was not as distinct.

Chiari Malformations

Sagittal MRI with a spin-echo technique (30 msec TE, 0.5 sec TR) accurately identified the type and severity of 10 Chiari malformations (nine Chiari I, one Chiari II) (fig. 2). The extent of cerebellar tonsil herniation, position of the fourth ventricle, and the relations of the brainstem and cervical medullary junction to the upper cervical canal and foramen magnum were sharply delineated. Hydrocephalus was noted in five and syringomyelia in two. Two patients were identified incidentally as having tonsillar herniation on sagittal brain MRI done for unrelated disorders.

Syringomyelia

Seven cases of syringomyelia were studied. Two had concomitant Chiari I malformations. In all cases, the cystic central cavity was identified to at least C6 (fig. 3A). One patient had syringobulbia; in three others, communication of the cavity with the fourth ventricle could be identified. The transverse diameter of the cord was increased in all cases (fig. 3B). On the spin-echo images (30 msec TE, 0.5 sec TR), the central

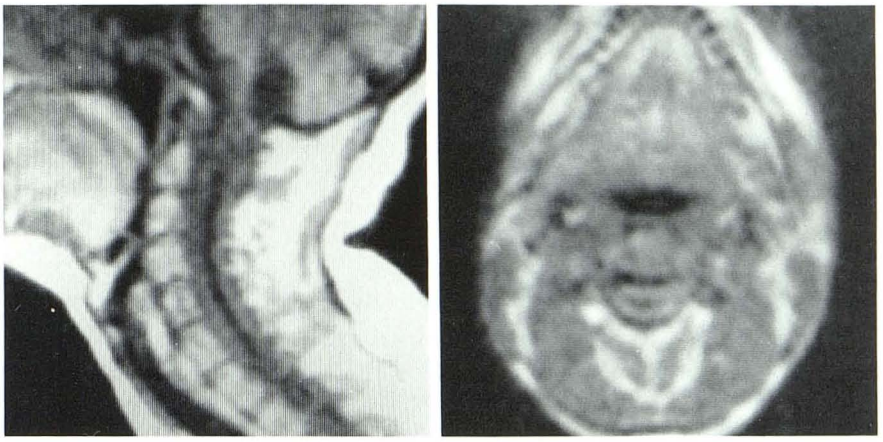

Fig. 3.—Syringomyelia. **A**, Spin-echo image (30 msec TE, 0.5 sec TR, 0.3 T superconductive unit) in sagittal plane. Well defined central area of decreased signal intensity extends throughout course of cervical cord. Downward displacement of fourth ventricle; hydrocephalus. **B**, Spin-echo image (30 msec TE, 0.5 sec TR, 0.3 T superconductive unit) in transverse plane in another patient. Widened transverse diameter of cord and central area of decreased signal intensity.

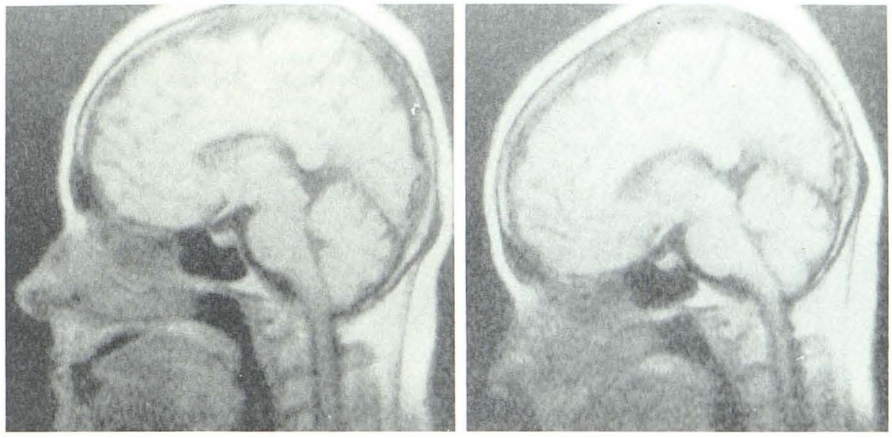

Fig. 4.—Influence of flexion on rheumatoid arthritis. Spin-echo images (30 msec TE, 0.5 sec TR, 0.15 T resistive unit). **A**, Supine neutral position. **B**, Supine flexion. Marked narrowing of foramen magnum by subluxation of C1 on C2.

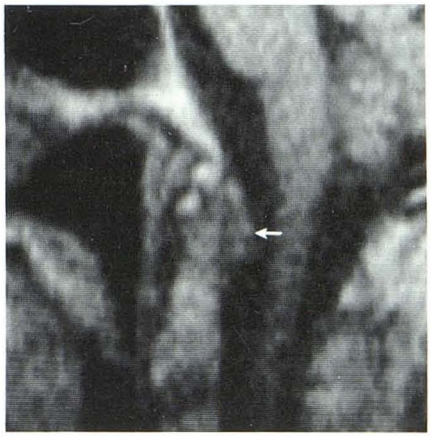

Fig. 5.—Rheumatoid arthritis. Spin-echo image (30 msec TE, 0.5 sec TR, 0.15 T resistive unit). Mass with soft-tissue signal intensity posterior to dens in region of joint synovium and transverse ligament (*arrow*).

cystic cavity appeared as an area of decreased signal intensity identical to CSF and clearly delineated from the cord. With longer TEs (60 or 120 msec) and TRs (>2 sec), the intensity of the CSF increased; delineation of the cavity from the cord was not as precise because the outline of the cord was less distinct.

Rheumatoid Arthritis

Two patients who had rheumatoid arthritis involving the cervical spine were studied. In one patient, flexion and extension sagittal MRI demonstrated subluxation of C1 on C2 comparable to the changes identified on the plain radiographs. The marked narrowing of the neural canal in the foramen magnum was better appreciated with MRI (fig. 4). In the second patient, a myelogram showed an extradural defect posterior to the dens. MRI was more specific in evaluating the nature of this defect. It demonstrated an apparent growth of the soft-tissue mass in the region of the joint synovium and transverse ligament posterior to the dens (fig. 5).

Degenerative Disease

There were 14 patients with degenerative disease. Thirteen had degenerative bony changes and/or a herniated disk diagnosed by myelography. One patient had a compression fracture of C5 and narrowing of the C5–C6 interspace.

With a spin-echo technique (30 msec TE, 0.5 sec TR) in the degenerative group, MRI depicted the herniated disk fragment and was as diagnostic as myelography in two cases (fig. 6). Incursions on the cervical cord or areas of canal narrowing were identified in 10 patients. In these patients, the changes were not as dramatic as the extradural defects seen on the myelogram, and the encroaching disk or bony spurs

6

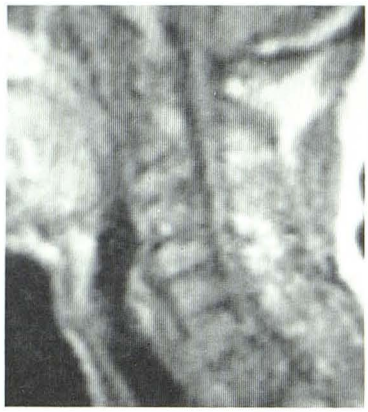

7A

7B

Fig. 6.—Herniated disk with complete block on myelography. Spin-echo image (30 msec TE, 0.5 sec TR, 0.15 T resistive unit). Mass of soft-tissue signal intensity posterior to C6–C7 level blocks neural canal (*arrow*). Because magnetic resonance image showed full craniocaudad extension of lesion, it was not necessary to instill contrast material from above. At surgery, large herniated disk fragment was removed.

Fig. 7.—Multiple extradural defects due to degenerative disease. **A**, Spin-echo image (30 msec TE, 0.5 sec TR, 0.3 T superconductive unit). Canal narrowing and incursions on anterior aspect of spinal cord. **B**, Pantopaque myelogram. Marked extradural defects at C3–C4, C4–C5, and C5–C6 levels.

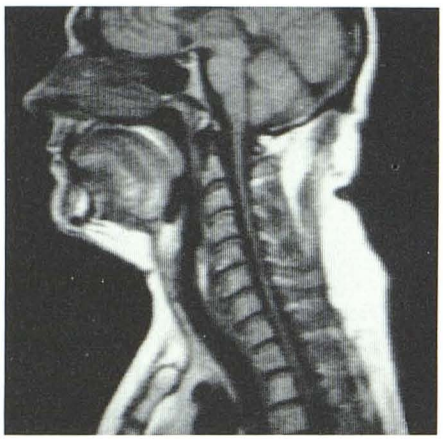

A

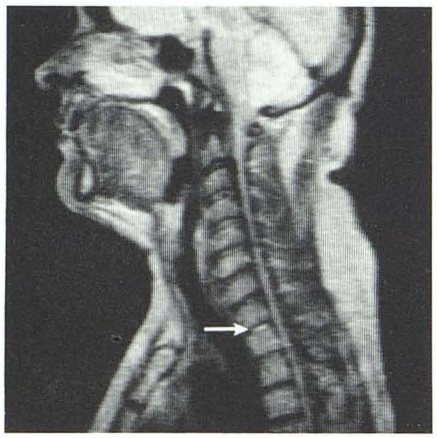

B

Fig. 8.—Multiple degenerative disk changes identified on plain films of cervical and thoracic spine. **A**, Spin-echo image (30 msec TE, 0.5 sec TR, 0.5 T superconductive unit). Variation in signal intensity of cervical and thoracic disks with subtle decreased signal intensity of C2, C5–C7, and T2–T4. **B**, Spin-echo image (60 msec TE, 2 sec TR, 0.5 T superconductive unit). With prolonged pulse technique, only disk of T1 demonstrates normal increased signal intensity of nucleus pulposus (*arrow*). Increased signal intensity of intracranial CSF.

were not directly seen (fig. 7). In one patient, a marked anterior extradural defect was identified on myelography, and the MRI study was normal.

In two patients where spin-echo techniques were performed with 60 msec TE, there was a decreased signal intensity of the disk at the involved levels. In one patient with extensive degenerative changes in the cervical and thoracic spine, all but one upper thoracic intervertebral disk showed decreased signal intensity (fig. 8).

In the patient with a traumatic compression fracture of C5, there was loss of volume of the vertebral body and C5–C6 interspace. There was a decreased signal intensity of the C5 disk when compared with the adjacent intervertebral disk. No deviation or incursion of the cervical cord was noted on MRI or on the myelogram.

Tumor

MRI identified mass lesions in two patients. One patient had a metastatic melanoma to the lower cervical spine (fig. 9). The second had a meningioma at the C2 level. The tumors were identified on spin-echo images (30 msec TE, 0.5 sec TR). The extent and location of the lesions were clearly depicted, and the level of the spinal canal block was accu-

A

B

Fig. 9.—Metastatic melanoma forming complete block at C7–T1 level. **A**, Myelogram. **B**, Spin-echo image (30 msec TE, 0.5 sec TR, 0.3 T superconductive unit) 1 cm left of midline. Tumor mass (*arrow*) at C6–C7 level. Spinal cord displaced to right, out of image plane from C5 through T1.

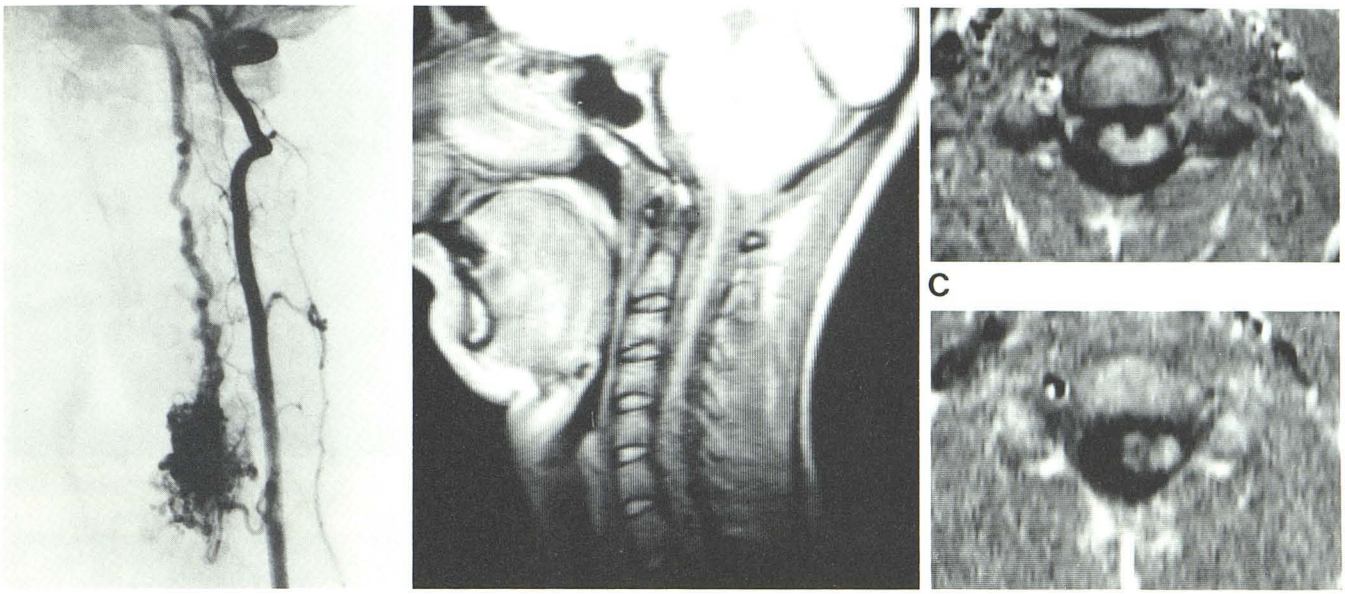

Fig. 10.—Arteriovenous malformation (AVM) in lower cervical region with large draining vein. **A**, Angiogram. **B**, Spin-echo image (60 msec TE, 2 sec TR). Cord is less distinct in lower cervical region as it is displaced to left. Mild anterior incursions on cord secondary to large draining vein. Increased signal intensity of CSF and intervertebral disks with this technique. **C**, Spin-echo transverse image (30 msec TE, 0.5 sec TR, 0.5 T superconductive unit) through superior part of AVM. Differentiation of CSF space, AVM, and spinal cord. AVM is on right lateral posterior aspect of cervical cord, displacing it to left. Central anterior incursion is from large draining vein. **D**, Inversion-recovery image (500 msec TI, 1.5 sec TR, 0.5 T superconductive unit) at different level. Displacement of cord to left is seen, but distinction of AVM from CSF space is not possible.

rately localized. However, with a short TE, the signal intensity of the lesions was similar to that of the spinal cord, and differentiation by signal intensity was not possible.

Miscellaneous

One patient with a cervical arteriovenous malformation (AVM) was studied in the sagittal and transverse planes with multiple pulse-sequence techniques (figs. 10A and 10B). Spin-echo images with TEs of 30, 60, and 120 msec and TRs of 0.5 and 2 sec and inversion-recovery images with TIs of 250, 500, and 800 msec and TRs of 1.5 and 2 sec were obtained. A spin-echo technique with a 30 msec TE and a 0.5 or 2 sec TR in the transverse plane differentiated the AVM from the CSF and the spinal cord by its intermediate signal intensity (figs. 10B and 10C). Inversion-recovery pulse sequences with 250 or 800 msec TI were unable to adequately distinguish the AVM from the adjacent CSF (fig. 10D).

The second patient in this category was a 36-year-old man with a history of multiple previous cervical laminectomies. A cystic mass lesion was identified posterior to the cord in the midcervical region. Spin-echo images with TEs of 30, 60, and 120 msec and TRs of 0.5 and 2 sec were obtained. The mass was thought to represent a traumatic subarachnoid cyst; increasing the TEs to 60 and 120 msec caused the signal intensity in it to increase markedly (fig. 11).

Discussion

MRI provides sharply defined anatomic delineation and tissue characterization. The contents of the posterior fossa and foramen magnum, the spinal cord, CSF, and extradural structures can be imaged in any plane without intrathecal contrast material or ionizing radiation. MRI is noninvasive, has a high patient tolerance, can be done on an outpatient basis, and offers no known biologic hazards at current magnetic field strengths and radiofrequency pulse sequences [6, 7].

Current Clinical Applications

Chiari malformations can be identified on an outpatient basis obviating myelography or CT with intrathecal contrast material. On the sagittal images, the type and extent of herniation can be evaluated, and the presence or absence of concomitant abnormalities such as hydrocephalus or syringomyelia is readily appreciated.

Syringomyelia is directly seen as an enlarged intramedullary CSF space with a spin-echo technique (30 msec TE, 0.5 sec TR). Distinction is made from an intramedullary soft-tissue mass, and identification of concomitant abnormalities such as a foramen magnum tumor or Chiari malformation is readily made. The cephalad and caudad extent and the character of the syrinx cavity are apparent. The opportunity to determine if the syrinx cavity communicates with the fourth ventricle is facilitated by the capability of multidimensional imaging without the degradation of images that occurs with secondary reconstruction in CT. In CT, even with the use of intrathecal contrast material and a delayed scan, the central cavity of syringomyelia is not as well defined.

MRI flexion and extension views of the cervical spine demonstrate not only the degree of subluxation that may be present, but also offer the advantage of direct depiction of

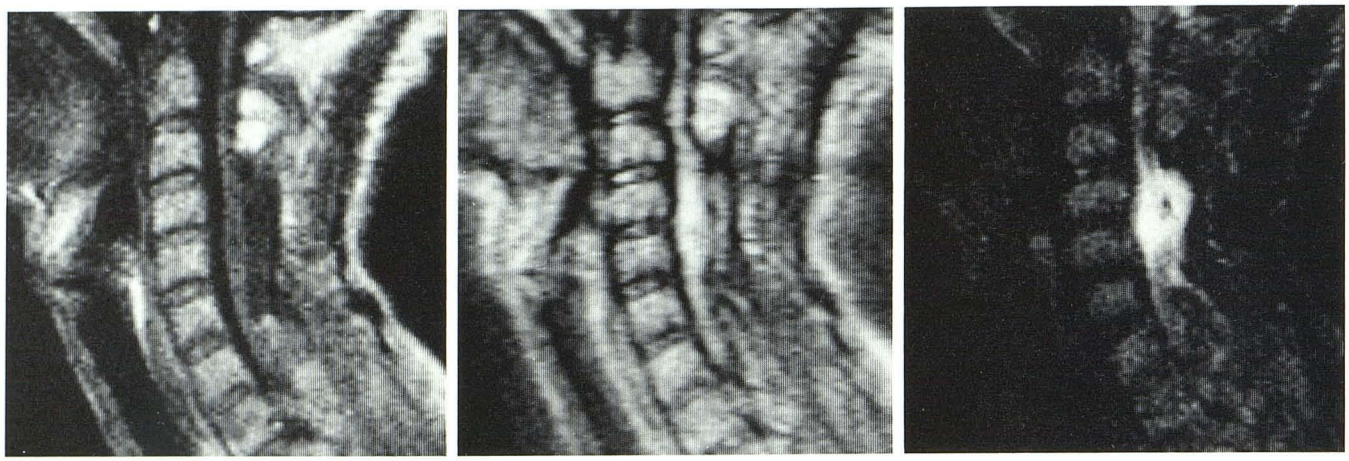

Fig. 11.—Postlaminectomy cystic mass. **A**, Spin-echo image (30 msec TE, 0.5 sec TR, 0.3 T superconductive unit). Cervical cord is fixed posteriorly at site of previous surgery. Cystic area of decreased signal intensity near and posterior to cervical cord. **B**, Prolonged spin-echo image (60 msec TE, 1 sec TR) through same area. Increased signal intensity to cystic region makes delineation from cervical cord less accurate. **C**, Long spin-echo image (120 msec TE, 2 sec TR). Marked increased signal intensity in cystic region typical of fluid.

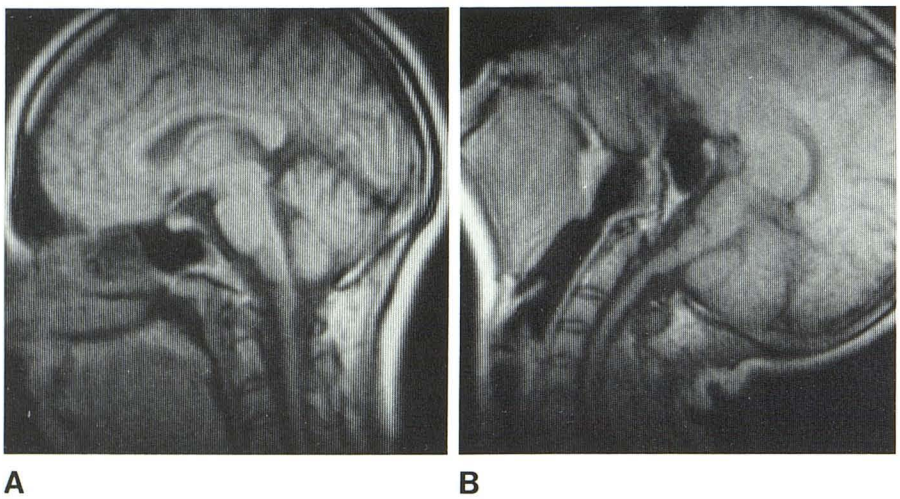

Fig. 12.—Normal spine with motion. Spin-echo images (30 msec TE, 0.5 sec TR, 0.15 T resistive unit). **A**, Neutral supine position. **B**, Extended prone position.

the spinal cord, surrounding CSF, and soft-tissue structures. This facilitates the evaluation of cord motion, impingement, and canal narrowing (figs. 4 and 12).

A mass lesion or spinal canal block, whether from an intra- or extradural process, is accurately localized and the extent defined, obviating contrast studies above and below the level of the lesion. Once identified, pulse-sequence changes may be needed to provide optimal distinction of the soft-tissue masses from the spinal cord outline on the basis of differences in signal intensity.

In the evaluation of degenerative disease of the spine, MRI was not as accurate as CT or myelography in this study. However, there are two potentially correctable factors to account for the difference between MRI and CT or myelography: patient position and slice thickness.

Contrast myelograms are made with the patient in the prone, neck-extended position. This results in a more anterior location of the spinal cord. With MRI, the patient is usually scanned in the supine, neutral position, and the cord lies more posteriorly. This may explain why anterior extra-dural lesions are not as obvious on MRI as on contrast myelograms. The extended prone position also can be used in MRI to bring the cord more anteriorly and accentuate any changes from anterior extradural lesions, such as hypertrophic degenerative changes or herniated disks (fig. 12).

Slice thickness is also a consideration. With our current MRI equipment, the thinnest sections are 1.0–1.5 cm, which causes partial-volume averaging and decreased spatial resolution. Thin sections and high spatial resolution are required for the evaluation of the neural foramina, nerve roots, and intervertebral disk spaces. CT remains more accurate at present. However, it has been our experience that increasing the magnetic field strength improves resolution. The signal-to-noise ratio of subcutaneous fat in the same patient was

measured with 0.15 and 0.35 T magnets. There was a linear improvement in the signal-to-noise ratio with increasing field strength. This agrees with the work of Hart [8] who found that the signal-to-noise ratio shows a linear improvement with increasing field strengths up to 1.5 T. With increased field strengths, it is possible to use thinner sections with MRI. This is an obvious advantage of superconductive systems over resistive units. Increasing field strength is more effective than increasing scan time in improving signal-to-noise ratio. With the latter, the signal-to-noise ratio improves only as the square root of the scan time. For example, images obtained with 0.35 T field-strength magnet for the same resolution would require only one-fourth the scan time of a 0.15 T system.

With current CT scanners, data acquisition time can be as little as 2 sec, and reconstruction time is less than 1 min in most scanners. With MRI, data acquisition time can be as long as 50 min depending on the TR and the strength of the magnet. At present, with our equipment, the shortest scan time is 20 min for the acquisition of eight contiguous slices.

Despite its current limitations, MRI has potential advantages in the evaluation of degenerative disease involving the spine. In particular, it seems to be more sensitive to disk degeneration and the identification of the normal nucleus pulposus than CT, myelography, or plain radiography.

Pulse-Sequence Considerations

One of the most important considerations in clinical magnetic resonance imaging is the pulse-sequence technique. Changes in the pulse-sequence technique can be used to enhance various tissue characteristics and provide information that is not available with standard imaging techniques such as CT, myelography, or plain radiography.

Inversion-recovery (IR) technique has superior T_1 contrast resolution to the spin-echo (SE) technique because it provides twice the dynamic range of magnetization. Therefore, IR has a greater sensitivity to small differences in T_1 as compared with SE for equal examination times. However, the use of IR technique will result in considerable lengthening (three- to fourfold) of the sequence-pulse interval. Hence, a smaller number of sequence interval acquisitions with IR are possible compared with an SE technique of equal examination time. This results in a decreased signal-to-noise ratio for IR and is evidenced clinically by decreased intensity of the signal of the spinal cord and disk tissue. Since the T_1s of CSF, fat, and spinal cord have large inherent differences, no significant advantage exists for the IR technique for purely anatomic delineation.

Our experience suggests that the spin-echo technique, with three different pulse-sequence variations, is the technique of choice for the evaluation of the spine. A short TE produces the best signal-to-noise ratio and spatial resolution. A longer TE maximizes the differences among the signal intensities of various tissues, and increasing both TR and TE produces a selective enhancement of the CSF signal intensity. The reason for these events is as follows:

The short-TE technique (30 msec TE, 0.5 sec TR) produces an image with less T_2 weighting but is useful because more projections are made in a given time, producing an improved signal-to-noise ratio. This is primarily because of the short TE and TR times. T_2 undergoes exponential decay, and there is exponential loss in the amount of T_2 signal with increasing TE. Further, shortening the TR will increase the number of samples that can be obtained in a given time, which also will improve the signal-to-noise ratio (fig. 13A).

This short-TE technique is used to diagnose and define Chiari malformations, mass lesions, and impingement on the cord at the level of the foramen magnum and in the spinal canal. This technique also provides sharp contrast resolution between soft-tissue structures such as the cord and the CSF space, allowing the demonstration of cavities within the cord as syringomyelia.

With the short-TE technique, the entire intervertebral disk is seen, but no distinction can be made between the anulus and the nucleus pulposus; changes occurring with disk degeneration are subtle. Incursions or deviation of the spinal cord from extradural defects are demonstrated, but the cause (e.g., a herniated disk or bony spur) may not be identified. Their signal intensity may be similar to CSF, or they may be obscured by partial-volume effects. With this technique, spinal-canal blocks or mass lesions such as tumors can be distinguished from the CSF, but their signal intensities may be similar to the spinal cord or extradural soft tissue, and distinction can be difficult.

An SE technique with a more *prolonged TE* and TR (60 or 120 msec TE, 1 sec TR) results in an image of a somewhat decreased signal-to-noise ratio for the same scan time but produces greater tissue contrast (figs. 13B and 13C). There is an optimal TE that produces maximal differences between two particular tissues, depending on T_1 and T_2 weighting.

A spin-echo technique with a short TR produces images that are more T_1 weighted because there is only partial T_1 relaxation between pulses. Increase of the TR decreases the relative T_1 contribution because there is more complete T_1 relaxation between pulses and, hence, a relative increase in T_2 contribution. Increasing the T_2 weighting is useful for distinguishing tumors from the spinal cord.

Increasing the TE is also useful for the evaluation of normal and degenerated disk. Normal nucleus pulposus, because of a higher water content than the anulus, has a higher signal intensity than the surrounding anulus. With degeneration, the water content of the nucleus pulposus decreases and produces an isodense image of the disk. The normal aging process of the disk also seems to result in similar changes. These changes are more obvious in the lumbar region where the volume of the nucleus pulposus is 10 times greater than in the cervical disk.

Degeneration of a disk is not necessarily an indication of herniation and can be seen in asymptomatic patients. However, all herniated disks are degenerated, and the loss of water content has been identified as early as 48 hr after herniation [9, 10]. If, on MRI, the nucleus pulposus is distinguished from the anulus, the disk is not degenerated and, hence, not herniated. MRI is more sensitive than CT to degeneration of the intervertebral disk, and the decrease in signal intensity representing a loss of water content can be

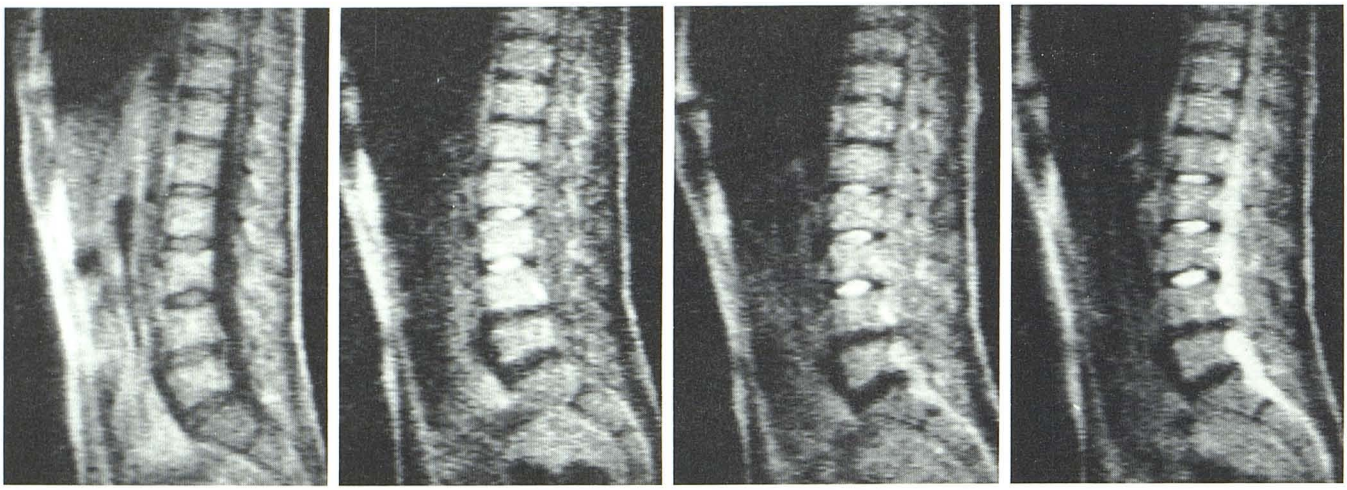

Fig. 13.—Herniated L4 disk. Effect of changing pulse technique. Metrizamide myelogram demonstrated large anterior extradural defect at L4 disk level. At surgery, large herniated L4 disk was identified. **A**, Short TE and TR image (30 msec TE, 0.5 sec TR, 0.15 T resistive unit). Good anatomic delineation. Minimal narrowing of L4–L5 interspace, but only subtle change in signal intensity of L4 and L5 disks when compared with L1, L2, or L3. **B**, Prolonged TE image (120 msec TE, 1 sec TR). Normal nucleus pulposus at L1–L3 shows increased signal intensity (white) and can be distinguished from anulus and surrounding cortical bone, which is of decreased signal intensity (black). L4 and L5 disks are degenerated, and nucleus pulposus, anulus, and cortical bone are isodense with decreased signal intensity. Slight increase in CSF signal intensity. **C**, Prolonged TE and TR image (120 msec TE, 2 sec TR). Further differentiation of normal nucleus pulposus at L1–L3 from surrounding anulus and cortical bone and decreased signal intensity of disks at L4 and L5 levels. **D**, Prolonged TE and longer TR image (120 msec TE, 3 sec TR). Marked increase in signal intensity of CSF; sharp delineation of extradural defect at L4 level from herniated disk. L5 disk is degenerated but not herniated.

identified before narrowing of the interspace occurs, the earliest change identifiable on plain radiographs. This is also useful in differentiating severe degenerative changes from infection. In a case of acute disk-space infection, the intervertebral disk and adjacent end plates had a markedly increased signal intensity because of inflammation using the prolonged TE technique. One disadvantage with this spin-echo technique is that there is a minimal increase in the intensity of the CSF, and this could obscure fluid cavities within the cord as in syringomyelia.

The need for a *lengthened TE and TR* sequence is because CSF, degenerated disk, and cortical bone can have similar signal intensities with most pulse sequences. Using the spin-echo technique with a prolonged TE and increasing the TR about to the T_1 of CSF or longer (about 1.5–2.5 sec) enhances the signal from CSF relative to the extradural structures. It is interesting to note that this change occurs at a shorter TR (about 1.5–2 sec) in the ventricles than in the spinal CSF space. This increase in uniform signal intensity of the CSF allows the identification of distortion of the subarachnoid space by impingement of the extradural structures, such as herniated disks or canal stenosis, providing an image comparable to a contrast myelogram (fig. 13D). The disadvantage of this technique when used by itself is that it will fail to differentiate the spinal cord and nerve roots from the CSF.

Different pulse-sequence techniques and multidimensional imaging with MRI add greatly to the flexibility of studying the spine on a single examination. Moreover, information comparable to that from CT, myelography, and plain radiography can be obtained in a noninvasive fashion without the use of ionizing radiation.

REFERENCES

1. DeLaPaz RL, Brady TJ, Buonanno FS, et al. Nuclear magnetic resonance (NMR) imaging of Arnold-Chiari type I malformation with hydromyelia. *J Comput Assist Tomogr* **1983**;7:126–129
2. Mills C, Brant-Zawadzki M, Crooks LE, Sheldon PE, Yates A. NMR imaging of the spine. Presented at the annual meeting of the American Roentgen Ray Society, Atlanta, April **1983**
3. Moon KL, Genant HK, Helms CA, Chafetz NI, Crooks LE, Kaufman L. Musculoskeletal applications of nuclear magnetic resonance. *Radiology* **1983**;147:161–171
4. Modic MT, Weinstein MA, Pavlicek W, et al. Nuclear magnetic resonance of the spine. *Radiology* **1983**;148:757–762
5. Rupp N, Reiser M, Stretter E. The diagnostic value of morphology and relaxation times in NMR-imaging of the body. *Eur J Radiol* **1983**;3:68–76
6. Budinger TF. Nuclear magnetic resonance (NMR) in vivo studies: known thresholds for health effects. *J Comput Assist Tomogr* **1981**;5:800–811
7. Thomas A, Morris PG. The effects of NMR exposure on living organisms. I. A microbial assay. *Br J Radiol* **1981**;54:615–621
8. Hart H. Technical alternatives to NMR imaging. Presented at the annual meeting of the American Roentgen Ray Society, Atlanta, April **1983**
9. Hendry NG. The hydration of the nucleus pulposus and its relation to invertebral disk derangement. *J Bone Joint Surg [Br]* **1958**;40:132–144
10. Lipson SJ, Muir H. Experimental intervertebral disc degeneration. *Arthritis Rheum* **1981**;24:12–21